SYMPOSIUM REPORT

# The 'window' T-type calcium current in brain dynamics of different behavioural states

Vincenzo Crunelli, Tibor I. Tóth, David W. Cope, Kate Blethyn and Stuart W. Hughes

*School of Biosciences, Cardiff University, Museum Avenue, Cardiff CF10 3US, UK*

**All three forms of recombinant low voltage-activated T-type $Ca^{2+}$ channels ($Ca_v3.1$, $Ca_v3.2$ and $Ca_v3.3$) exhibit a small, though clearly evident, window T-type $Ca^{2+}$ current ($I_{Twindow}$) which is also present in native channels from different neuronal types. In thalamocortical (TC) and nucleus reticularis thalami (NRT) neurones, and possibly in neocortical cells, an $I_{Twindow}$-mediated bistability is the key cellular mechanism underlying the expression of the slow ($< 1$ Hz) sleep oscillation, one of the fundamental EEG rhythms of non-REM sleep. As the $I_{Twindow}$-mediated bistability may also represent one of the cellular mechanisms underlying the expression of high frequency burst firing in awake conditions, $I_{Twindow}$ is of critical importance in neuronal population dynamics associated with different behavioural states.**

(Received 28 September 2004; accepted after revision 19 October 2004; first published online 21 October 2004)
**Corresponding author** V. Crunelli: School of Biosciences, Cardiff University, Museum Avenue, Cardiff CF10 3US, UK. Email: crunelli@cardiff.ac.uk

## Introduction

Low voltage-activated T-type $Ca^{2+}$ channels are an important component of the large array of voltage-dependent membrane channels used by neurones to express different network dynamics. Their characteristic voltage dependence and kinetics allow them to generate a transient, depolarizing, low-threshold $Ca^{2+}$ spike or potential (LTCP) which in turn evokes a peculiar firing pattern consisting of a high frequency (100–400 Hz) burst of action potentials (Huguenard, 1996; Perez-Reyes, 2003). Since the work of Llinas's group in Purkinje (Llinas & Sugimori, 1980*a*,*b*) and inferior olive neurones (Llinas & Yarom, 1981*a*,*b*), the physiological expression of neuronal T-type $Ca^{2+}$ channels has now been demonstrated in different neurones and has become synonymous with LTCP generation and burst firing.

Recent work in thalamic neurones indicates that neuronal T-type $Ca^{2+}$ channels also underlie membrane potential bistability, i.e. the existence of two resting membrane potentials. This neuronal property is due to the *window current* generated by these channels, i.e. $I_{Twindow}$ (Williams *et al.* 1997; Toth *et al.* 1998). Here, we summarize the biophysics underlying the physiological expression of $I_{Twindow}$, and describe how the $I_{Twindow}$-mediated bistability in thalamic neurones is a key component in the generation of the slow ($< 1$ Hz) sleep rhythm (Hughes *et al.* 2002), one of the fundamental EEG activities in non-REM sleep dynamics (Steriade *et al.* 1993*d*). In a prospective outlook we will then consider how neuronal $I_{Twindow}$ may underlie other activities during the awake state. The distinct and important physiological roles that $I_{Twindow}$ plays in non-neuronal cells have been reviewed elsewhere (Lambert *et al.* 2001; Perez-Reyes, 2003).

## Biophysics of $I_{Twindow}$

The window (or steady-state) component of an inactivating, voltage-dependent membrane current originates from the region of overlap (shaded in grey in Fig. 1*Aa*) between its steady-state activation and inactivation curves. In this voltage region, there is a fraction of channels which do not fully inactivate and therefore remain open. The estimated magnitude of the window current is strongly dependent on the steepness of these curves and their relative position with respect to the voltage axis (Fig. 1*Aa*). Since the activation and inactivation curves are obtained by fitting exponential functions to experimental measurements that in this voltage region are very small and highly dependent on the experimental conditions, great caution should be used in interpreting data on window currents. Furthermore, because these curves decay exponentially towards the

In memory of Eberhard H. Buhl. This report was presented at The Journal of Physiology Symposium in honour of the late Eberhard H. Buhl on Structure/Function Correlates in Neurons and Networks, Leeds, UK, 10 September 2004. It was commissioned by the Editorial Board and reflects the views of the authors.

 DOI: 10.1113/jphysiol.2004.076273

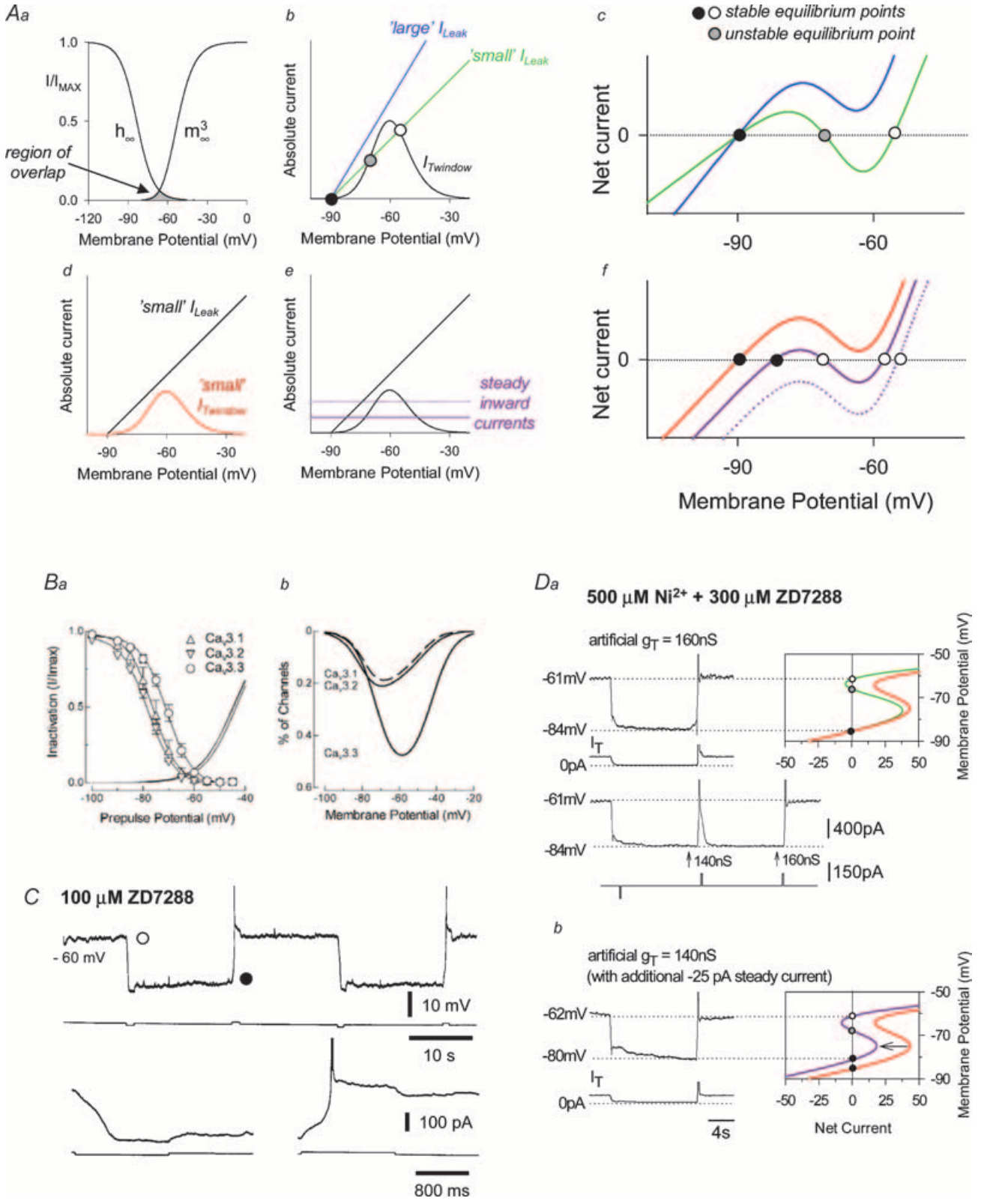


**Figure 1. Biophysics of $I_{Twindow}$-mediated bistability and its demonstration in TC neurones**
*Aa*, steady-state activation and inactivation curves of $I_T$ from a TC neurone *in vitro*, showing in grey the region of overlap, i.e. the basis for $I_{Twindow}$. *b*, plot of the *absolute value* of $I_{Twindow}$ (bell-shaped curve) and two $I_{leak}$s (blue and green lines). *c*, net current–voltage plot for the colour coded conditions depicted in *b*: bistability, i.e. two stable membrane potentials (filled and open circle), is present for the green but not for the blue line. *d*, plot of

voltage axis (i.e. they tend to zero at infinity) (Fig. 1*Aa*), all inactivating currents, including those with steady-state activation and inactivation curves that are far apart and shallow, possess a window current, even if extremely small. As has been the case for other inactivating currents, therefore, the issue is not whether neuronal $I_{Twindow}$ exists, but rather whether it has any physiological role, i.e. whether the small fraction of 'non-inactivating' neuronal T-type $Ca^{2+}$ channels responsible for $I_{Twindow}$ makes any contribution to single neurone activities and neural network dynamics.

A small, but clearly discernable, $I_{Twindow}$ was evident in the first studies that investigated native neuronal T-type $Ca^{2+}$ channels (Carbone & Lux, 1984; Nowycky *et al.* 1985; Fox *et al.* 1987). Since then, $I_{Twindow}$ has been observed in many neuronal types (including the thalamic neurones on which this review will focus) (Coulter *et al.* 1989; Crunelli *et al.* 1989; Hernandez-Cruz & Pape, 1989) (Fig. 1*Aa*), using different preparations and techniques in both young and adult animals of different species (Huguenard, 1996; Perez-Reyes, 2003). From these data, $I_{Twindow}$ may be estimated to be generated by 0.05–0.8% of the total number of T-type channels in different CNS neurones. Recent investigations on recombinant $Ca_v3.1$, $Ca_v3.2$ and $Ca_v3.3$ channels (derived from the respective $\alpha$1G, $\alpha$1H and $\alpha$1I pore forming subunits) have confirmed the results on native channels (Fig. 1*Ba*), and highlighted a larger $I_{Twindow}$ for $Ca_v3.3$ channels than for the other two types (Klockner *et al.* 1999) (Fig. 1*Bb*). These data are particularly important for thalamic cells, since glutamatergic thalamocortical (TC) neurones mostly express $Ca_v3.1$ and a very small number of $Ca_v3.2$ channels, whereas the GABAergic neurones of the nucleus reticularis thalami (NRT) are mainly endowed with $Ca_v3.3$ and much smaller amounts of $Ca_v3.1$ and $Ca_v3.2$ channels (Talley *et al.* 1999; Perez-Reyes, 2003).

### Neuronal $I_{Twindow}$ and membrane potential bistability

The *transient activation* of neuronal T-type $Ca^{2+}$ channels generates the characteristic LTCP and associated high frequency burst firing. In contrast, the *non-inactivating* fraction of T-type $Ca^{2+}$ channels leads, in the generally small membrane potential region of their expression, to a 'steady' influx of $Ca^{2+}$ into the neurone, and thus to a 'non-inactivating' inward current ($I_{Twindow}$) and a resulting 'tonic' depolarization. To fully appreciate the physiological significance of $I_{Twindow}$ in neuronal activity, however, it is necessary to consider the interaction between this current and the leak $K^+$ current ($I_{leak}$) in the absence of other membrane currents. In Fig. 1*Ab*, the absolute amplitude of $I_{Twindow}$ (bell-shaped curve) has been plotted against the membrane potential, while two $I_{leak}$s are represented by the blue and green lines. When the slope of $I_{leak}$ (i.e. $g_{leak}$) is relatively small (green line in Fig. 1*Ab*), $I_{leak}$ crosses the bell-shaped $I_{Twindow}$ curve in three points, at which both currents have equal values. Since $I_{Twindow}$ is an inward and $I_{leak}$ an outward current, these are three points of zero net current (Fig. 1*Ac*): the leftmost and rightmost points are stable equilibrium points (filled and open circles on green line in Fig. 1*Ac*, respectively) whilst the middle point is unstable (i.e. grey circle in Fig. 1*Ac*). Under this condition the system generated by $I_{Twindow}$ and $I_{leak}$ is bistable and, in the absence of other currents in this voltage region, neurones show two stable resting membrane potentials: one depolarized state where $I_{Twindow}$ is 'on' (open circle on green line in Fig. 1*Ac*) and a hyperpolarized state where $I_{Twindow}$ is 'off' (filled circle on green line in Fig. 1*Ac*). In contrast, when $g_{leak}$ is relatively large (blue line in Fig. 1*Ab*) $I_{leak}$ crosses the $I_{Twindow}$ curve only in one point, which represents the resting membrane potential (filled circle on blue line in Fig. 1*Ac*).

Clearly, changes in $I_{leak}$ are not the only modifications that can bring about or remove $I_{Twindow}$-mediated bistability. As shown in Fig. 1*Ad*, bistability is lost when a small $I_{leak}$ interacts with a small $I_{Twindow}$, which may result either from a reduction in $g_T$, rightward and leftward shifts in its steady-state activation and inactivation curve, respectively, or a decrease in their steepness. This would give rise to a single equilibrium point (filled circle on red line in Fig. 1*Af*). Also important, both from a biophysical and physiological perspective, are

the small $I_{leak}$ as in *b* and a small $I_{Twindow}$ (red curve) shows only one point of intersection. *e*, plot of the small $I_{leak}$ and $I_{Twindow}$ as in *d*, but with two steady inward currents (continuous and dashed purple lines). *f*, net current–voltage plot for the colour coded conditions depicted in *d* and *e*: bistability is absent when $I_T$ is small (red line), but can be reintroduced by addition of a steady inward current that shifts the curve downwards (continuous purple line). A larger inward current further shifts the curve downwards with a loss of bistability and an instatement of a more depolarized membrane potential (open circle on dashed purple line). *B*, steady-state activation and inactivation curves for recombinant $Ca_v3.1$, $Ca_v3.2$ and $Ca_v3.3$ channels (*a*), and corresponding window currents (*b*). *C*, bistability is observed in TC neurones when $I_h$ is blocked with ZD 7288. The transition from one to the other resting potential is achived by intracellular injection of current pulses. *Da*, following the block of $I_T$ with $Ni^{2+}$, bistability is reintroduced in this TC neurone by using an amount of computer-generated $I_T$ commensurate with the theoretical prediction (i.e. the unfilled and filled circles of the green line in the voltage-net current plot match the two experimentally measured resting membrane potentials). A decrease in artificial $g_T$ to 140 nS (bottom records) abolishes the bistability as the voltage–net current plot now has only one resting membrane potential (filled circle of red line), as shown in *Ab* and *Ad*. However, using the same $g_T$, bistability is reintroduced by the addition of a steady direct current (continuous purple line), as shown in *Ae* and *Af*. *B* used from Perez-Reyes, (2003) with permission (©2003, American Physiological Society).

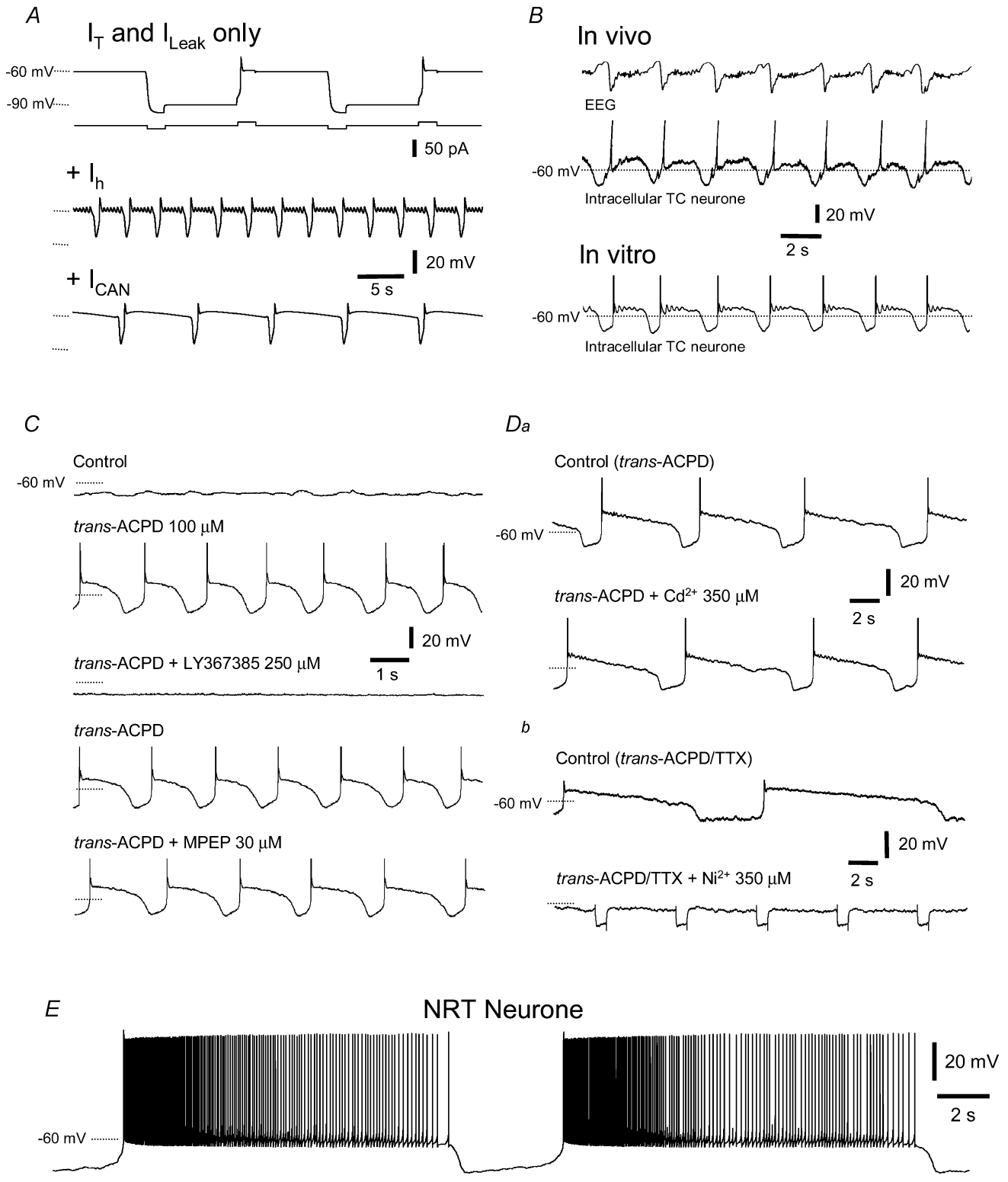


**Figure 2. $I_{Twindow}$-mediated bistability is the key cellular mechanism of the slow (< 1 Hz) sleep oscillation in TC and NRT neurones**

*A*, bistability in computer simulations using a TC neurone model containing only $I_T$ and $I_{leak}$ (upper trace). Note the similarity of the waveform to the experimental records in Fig. 1*C*. Addition of $I_h$ leads to a continuous oscillation of the membrane potential (middle trace), the period of which is drastically affected by the further addition of $I_{CAN}$ to the model (lower trace). *B*, similarities of the slow (< 1 Hz) sleep oscillation observed *in vitro* and *in vivo* (the latter recorded simultaneously with the slow (< 1 Hz) rhythm in the EEG. *C*, in every TC neurone *in vitro*,

the cases where in the absence of any change in both $I_{Twindow}$ and $I_{leak}$, bistability can be instated or eliminated by addition of a tonic current (Fig. 1*Ae*). For example, in the non-bistable system of Fig. 1*Ad*, addition of a steady inward current (continuous purple line in Fig. 1*Ae*) would shift the entire net current–voltage curve downwards (continuous purple line in Fig. 1*Af*), thus reintroducing bistability. Addition of a larger steady inward current (dashed purple line in Fig. 1*Ae*) would then remove bistability, moving the curve even further downwards and thus allowing only one resting membrane potential to exist (open circle on dashed purple line in Fig. 1*Af*).

### Physiological expression of $I_{Twindow}$

Experimental confirmation of the presence of a physiologically relevant $I_{Twindow}$ has come from work in rat and cat TC neurones (Williams *et al.* 1997; Hughes *et al.* 1999; Hughes *et al.* 2002), of different sensory and motor thalamic nuclei (Blethyn *et al.* 2002), and NRT neurones (Blethyn *et al.* 2003). In these neurones bistability is observed after appropriate block of $I_h$ (the most prominent current present within the voltage region where $I_{Twindow}$ is expressed), and, as predicted, appropriate voltage steps are able to switch the membrane potential between the two stable states (Williams *et al.* 1997) (Fig. 1*C*). This bistability is unaffected by $Ba^{2+}$ and blockers of high threshold $Ca^{2+}$ currents, including $Cd^{2+}$, but is abolished by relatively small concentrations of $Ni^{2+}$ (see Fig. 2*D*). The preferential block by $Ni^{2+}$, compared to the lack of effect by similar concentrations of $Cd^{2+}$, indicates that bistability is dependent on $I_T$.

Additional and conclusive evidence for the involvement of $I_{Twindow}$ in the membrane potential bistability of thalamic neurones is provided by appropriately manipulating $I_T$ (and thus $I_{Twindow}$) using the dynamic clamp (Hughes *et al.* 1999, 2002), a technique that allows a computer-generated current to be either added to, or subtracted from a living neurone (Sharp *et al.* 1993). Thus, in an originally bistable TC neurone where $I_T$ (and thus bistability) had been pharmacologically eliminated by $Ni^{2+}$, bistability can be reinstated by adding an amount of computer-generated $I_T$ commensurate with the apparent $I_{leak}$ of that neurone, such that the net current–voltage plot for that neurone satisfies the theoretical prediction (green line in Fig. 1*Da*). Similar dynamic clamp experiments (Hughes *et al.* 1999) also demonstrate that TC neurones lose their bistable properties by changes in artificial $I_T$ that decrease the size of $I_{Twindow}$, for instance by moving apart the steady-state activation and inactivation curves of the computer generated $I_T$ by as little as 5 mV, or by reducing $g_T$ (red line in Fig. 1*Da*, see also Fig. 1*Ad* and A*f*). In the latter case, bistability could then be re-introduced by an appropriate change in direct current (continuous purple line in Fig. 1*Ab*), as explained in the previous section (see Fig. 1*Ae* and *Af*).

### $I_{Twindow}$-mediated bistability is the cellular mechanism of the slow sleep ($\leq$ 1 Hz) oscillation

As shown by computer simulations, addition of the hyperpolarization-activated current ($I_h$) drastically transforms the $I_{Twindow}$–$I_{leak}$ bistable system into a continuous oscillation of the membrane potential (Fig. 2*A*), by introducing a voltage-dependent, non-inactivating inward current. The period, and other properties of this oscillation, are also critically controlled by the presence of a $Ca^{2+}$-dependent, non-selective cation current ($I_{CAN}$) (Hughes *et al.* 2002) (Fig. 2*A*).

This $I_{Twindow}$-mediated, membrane potential oscillation is indeed the activity that is observed in TC and NRT neurones when $I_h$ is not blocked (Fig. 2*B*). Extensive *in vitro* and *in vivo* studies (Hughes *et al.* 2002, 2004) have now shown it to represent the slow ($< 1$ Hz) sleep oscillation, i.e. the intracellularly recorded thalamic counterpart of the slow ($< 1$ Hz) sleep rhythm recorded in the EEG (Steriade *et al.* 1993*a*; Contreras & Steriade, 1995) (Fig. 2*B*). Both in animals (Steriade *et al.* 1993*b*) and in humans (Achermann & Borbely, 1997), this rhythm is one of the fundamental components of sleep dynamics during non-REM sleep, and a single slow ($< 1$ Hz) sleep oscillation cycle within the thalamocortical loop is now believed to underlie the expression of a K-complex in the EEG (Amzica & Steriade, 1997).

The bistability, and the slow ($< 1$ Hz) sleep oscillation, however, can be seen *in vitro* only in a very small proportion (15%) of TC neurones under control conditions (Williams *et al.* 1997), but in 56% of TC neurones following electrical stimulation of the cortical afferents present in the slice (Hughes *et al.* 2002). Similarly, none of the TC neurones *in vivo* expresses the slow ($< 1$ Hz) oscillation following removal of the

the non-selective mGluR agonist (+/−)-1-aminocyclopentane-trans-1,3-dicarboxylic acid (*trans*-ACPD) elicits the slow ($< 1$ Hz) sleep oscillation, which is unaffected by the selective mGluR5 antagonist 2-methyl-G-(phenylethynyl) pyridine (MPEP), but blocked by the selective mGluR1a antagonist LY367385. *D*, block of the slow ($< 1$ Hz) sleep oscillation by $Ni^{2+}$ but not by $Cd^{2+}$. Downward deflections in the lowermost record are the neurone response to hyperpolarizing current pulses. *E*, the slow ($< 1$Hz) sleep oscillation recorded in an NRT neurone *in vitro*. *B* from contreras & Steriade (1995) with permission (© 1995 by the Society for Neuroscience). *C* and *D* from Sherman *et al.* (2001) with permission (© 2002, Elsevier).

cortex (a condition similar to the *in vitro* situation), but the majority shows it when the cortex is left intact (Timofeev & Steriade, 1996). Together these *in vitro* and *in vivo* results show that the corticofugal afferents to TC neurones strongly contribute to setting the $I_{Twindow}$–$I_{leak}$ system to become bistable, either by changing $I_{leak}$ or $I_{Twindow}$, or adding/removing a tonic input (as shown schematically in Fig. 1*Ab*, *d* and *e*, respectively). In TC neurones that are non-oscillating in control conditions *in vitro*, the simple addition of direct current does not bring about the slow (< 1 Hz) sleep oscillation, and an increase in $g_T$ or a modification of its voltage region of expression (by manipulating the relative position of the steady-state activation and inactivation curves of computer-generated $I_T$) does not satisfactorily reproduce *all* the properties of the slow (< 1 Hz) oscillation (Hughes *et al.* 1999). On the other hand, dynamic clamp experiments that decrease $I_{leak}$ show an oscillation with identical characteristics to the one observed *in vivo* (Hughes *et al.* 1999). Indeed, it is the synaptic activation of metabotropic glutamate receptors (mGluR1a) that instates the decrease in $I_{leak}$ necessary for establishing the $I_{Twindow}$–$I_{leak}$ bistable system, as also demonstrated *in vivo* and *in vitro* using selective mGluR agonists and antagonists (Hughes *et al.* 2002, 2004) (Fig. 2*C*).

Figure 3 summarizes the cellular mechanism of the slow (< 1 Hz) sleep oscillation in TC neurones, where (i) $I_{Twindow}$ plays the major role by setting the level of the up ($I_{Twindow}$ 'on') and down ($I_{Twindow}$ 'off') states of the oscillation, (ii) $I_h$ is responsible for repolarizing the neurone from the down state and thus critically determines the duration of the down state, and (iii) $I_{CAN}$ tightly controls the duration of the up state and is thus responsible for stabilizing the voltage region of existence of the slow oscillation (see Fig. 8 in Hughes *et al.* 2002). A very similar mechanism underlies the slow (< 1 Hz) sleep oscillation in NRT neurones (Fig. 2*E*), with $I_{Twindow}$ setting the basic levels for its up and down states (Blethyn *et al.* 2003).

### $I_{Twindow}$-mediated bistability as a potential cellular mechanism of the high frequency bursts in the awake state

In the awake state, TC neurones are considerably more depolarized than during sleep, a situation similar to that depicted by the dashed purple line in Fig. 1*Af* where only one membrane potential exists (open circle) and bistability is not present. Computer simulations and *in vitro* experiments, however, have shown that even when the membrane potential of TC neurones is

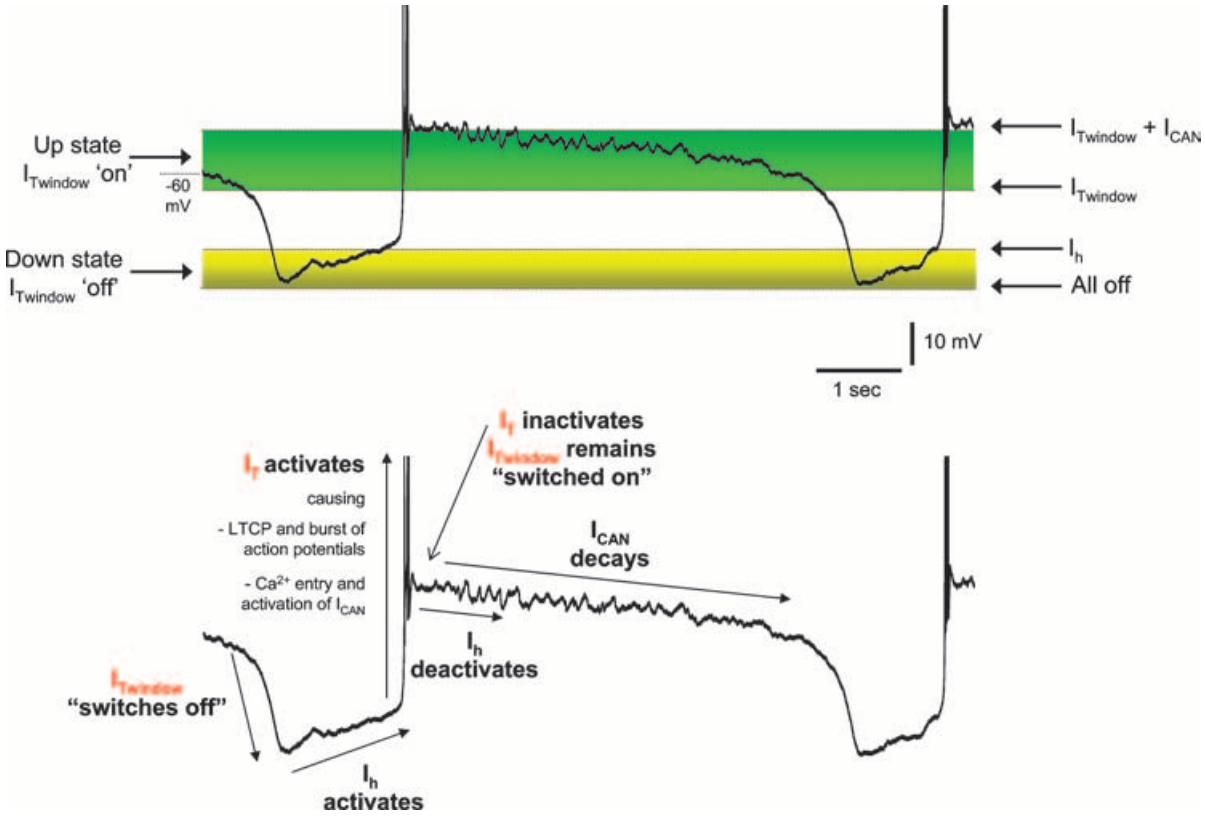


**Figure 3. Summary of the $I_{Twindow}$-mediated cellular mechanism of the slow (< 1 Hz) sleep oscillation in TC neurones**

$> -60$ mV, a small EPSP (or IPSP) can temporarily bring the membrane potential into the voltage region where the $I_{Twindow}$-mediated bistable mechanism could become transiently operational. This results in a stereotypical response consisting of a hyperpolarization (i.e. switching off of $I_{Twindow}$) that is always terminated by an LTCP and associated high frequency burst firing (Fig. 4*A* and *B*), thus amplifying the output of TC neurones to small-amplitude, isolated, subthreshold synaptic potentials (Williams *et al.* 1997).

High frequency bursts have been shown to occur sporadically in some TC neurones of awake rats (Fanselow *et al.* 2001), guinea pigs (Massaux & Edeline, 2003), rabbits (Swadlow & Gusev, 2001), cats (Guido & Weyand, 1995) and monkeys (Ramcharan *et al.* 2000) (Fig. 4*C*), and often as part of the initial, though delayed, response to a sensory stimulus (Sherman, 2001). Although these bursts have been suggested to arise from the activation of T-type $Ca^{2+}$ channels, no mechanism has been put forward to explain how this can occur from the relatively depolarized membrane potential that TC neurones occupy in the awake state. The $I_{Twindow}$-mediated amplification described above might be one such explanation. In this scenario, the delay and the strength of the LTCP-mediated action potential burst would not be strictly set, but could be finely tuned by (i) the neurone's $I_{leak}$, which takes into account the overall background synaptic activity (Destexhe *et al.* 2001), (ii) the strength of $I_h$, which is known to be modulated by many thalamic transmitters (McCormick, 1992), and (iii) the number of T-type $Ca^{2+}$ channels available for activation, which paradoxically is larger following a relatively prolonged period of depolarization (Leresche *et al.* 2004).

## Perspective outlook

The presence of $Ca_v3.1$, $Ca_v3.2$ and $Ca_v3.3$ channels in neurones of almost any brain region (Perez-Reyes, 2003) would support the notion that similar $I_{Twindow}$-mediated activities as those described above for thalamic neurones may occur in various neuronal types throughout the brain. In particular, the $I_{Twindow}$-mediated bistability might be the fundamental mechanism underlying the slow ($< 1$ Hz) sleep oscillation in neocortical cells (Steriade *et al.* 1993*c*), upon which synaptic influences would undoubtedly exert their modulation (Sanchez-Vives & McCormick, 2000).

Although we have concentrated here on the electrical behaviours that occur as a result of the $I_{Twindow}$-mediated bistability, one should not discard the potential presence of other physiologically relevant effects of $I_{Twindow}$ that are specifically linked to $Ca^{2+}$ influx, for example the modulation of biochemical pathways and gene expression. With the known role of intracellular $Ca^{2+}$ in short- and long-term neuronal plasticity, these actions could be of particular significance for thalamic and cortical neurones in view of recent data on the effect of the deep stages of non-REM sleep on memory (Huber *et al.* 2004).

The discovery of a physiological role for $I_{Twindow}$ in thalamic neurones, and its likely involvement in the activities of many other neuronal types, clearly raise the question of potential alterations of this component of $I_T$ in neurological and psychiatric disorders. These could

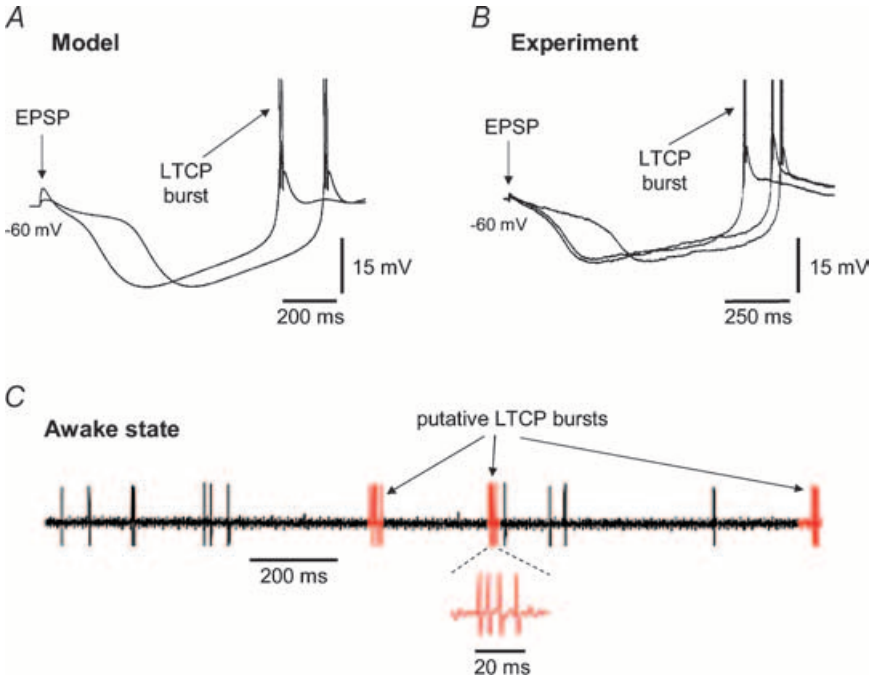


**Figure 4. The $I_{Twindow}$-mediated bistable system may be responsible for high frequency burst firing in TC neurones during the awake state**
*A*, computer simulations showing how at $-60$ mV two small EPSPs can evoke the stereotypical $I_{Twindow}$-mediated response, consisting of a large hyperpolarization followed by an LTCP and high frequency firing. *B*, the same sequence of events as in *A* can be recorded *in vitro* in TC neurones. *C*, extracellular activity from a TC neurone of an awake behaving monkey showing high frequency bursts with putative characteristics of an LTCP-mediated event. *C* from Sherman (2001) with permission (©2001, Elsevier).

either be primary changes in $I_T$ that might contribute to pathophysiological conditions (Tsakiridou *et al.* 1995) or alterations in $I_T$ that are secondary to other abnormalities, such as extracellular pH changes (Shah *et al.* 2001), genetic mutations of other $Ca^{2+}$ channels (Zhang *et al.* 2002), or continuous paroxysmal firing (Su *et al.* 2002).

## References


Achermann P & Borbely AA (1997). Low-frequency (< 1 Hz) oscillations in the human sleep electroencephalogram. *Neuroscience* **81**, 213–222.

Amzica F & Steriade M (1997). The K-complex: its slow (<1-Hz) rhythmicity and relation to delta waves. *Neurology* **49**, 952–959.

Blethyn KL, Hughes SW, Cope DW & Crunelli V (2002). Nucleus-specific properties of the slow (<1 hz) oscillation in thalamic neurones *in vitro*. *Soc Neurosci Abstr* **28**, 352.4.

Blethyn KL, Hughes SW, Cope DW & Crunelli V (2003). The role of ionic conductances underlying a slow (<1 hz) oscillation in neurones of the thalamic reticular nucleus *in vitro*. *Soc Neurosci Abstr* **29**, 699.3.

Carbone E & Lux HD (1984). A low voltage-activated, fully inactivating Ca channel in vertebrate sensory neurones. *Nature* **310**, 501–502.

Contreras D & Steriade M (1995). Cellular basis of EEG slow rhythms: a study of dynamic corticothalamic relationships. *J Neurosci* **15**, 604–622.

Coulter DA, Huguenard JR & Prince DA (1989). Calcium currents in rat thalamocortical relay neurones: kinetic properties of the transient, low-threshold current. *J Physiol* **414**, 587–604.

Crunelli V, Lightowler S & Pollard CE (1989). A T-type $Ca^{2+}$ current underlies low-threshold $Ca^{2+}$ potentials in cells of the cat and rat lateral geniculate nucleus. *J Physiol* **413**, 543–561.

Destexhe A, Rudolph M, Fellous JM & Sejnowski TJ (2001). Fluctuating synaptic conductances recreate *in vivo*-like activity in neocortical neurons. *Neuroscience* **107**, 13–24.

Fanselow EE, Sameshima K, Baccala LA & Nicolelis MA (2001). Thalamic bursting in rats during different awake behavioral states. *Proc Natl Acad Sci U S A* **98**, 15330–15335.

Fox AP, Nowycky MC & Tsien RW (1987). Single-channel recordings of three types of calcium channels in chick sensory neurones. *J Physiol* **394**, 173–200.

Guido W & Weyand T (1995). Burst responses in thalamic relay cells of the awake behaving cat. *J Neurophysiol* **74**, 1782–1786.

Hernandez-Cruz A & Pape HC (1989). Identification of two calcium currents in acutely dissociated neurons from the rat lateral geniculate nucleus. *J Neurophysiol* **61**, 1270–1283.

Huber R, Ghilardi MF, Massimini M & Tononi G (2004). Local sleep and learning. *Nature* **430**, 78–81.

Hughes SW, Cope DW, Blethyn KL & Crunelli V (2002). Cellular mechanisms of the slow (<1 Hz) oscillation in thalamocortical neurons in vitro. *Neuron* **33**, 947–958.

Hughes SW, Cope DW, Toth TI, Williams SR & Crunelli V (1999). All thalamocortical neurones possess a T-type $Ca^{2+}$ 'window' current that enables the expression of bistability-mediated activities. *J Physiol* **517**, 805–815.

Hughes SW, Lorincz M, Cope DW, Blethyn KL, Kekesi KA, Parri HR *et al*. (2004). Synchronized oscillations at alpha and theta frequencies in the lateral geniculate nucleus. *Neuron* **42**, 253–268.

Huguenard JR (1996). Low-threshold calcium currents in central nervous system neurons. *Annu Rev Physiol* **58**, 329–348.

Klockner U, Lee JH, Cribbs LL, Daud A, Hescheler J, Pereverzev A *et al*. (1999). Comparison of the $Ca^{2+}$ currents induced by expression of three cloned alpha1 subunits, alpha1G, alpha1H and alpha1I, of low-voltage-activated T-type $Ca^{2+}$ channels. *Eur J Neurosci* **11**, 4171–4178.

Lambert RC, Leresche N, Kozlov AS, Hering J, Maulet Y, Richard S *et al*. (2001). Les entrées de calcium au voisinage du potentiel de repos: un rôle sur mesure pour les canaux T dans de multiples fonctions. *Médicine/Science* **17**, 989–998.

Leresche N, Hering J & Lambert RC (2004). Paradoxical potentiation of neuronal T-type $Ca^{2+}$ current by ATP at resting membrane potential. *J Neurosci* **24**, 5592–5602.

Llinas R & Sugimori M (1980*a*). Electrophysiological properties of *in vitro* Purkinje cell dendrites in mammalian cerebellar slices. *J Physiol* **305**, 197–213.

Llinas R & Sugimori M (1980*b*). Electrophysiological properties of *in vitro* Purkinje cell somata in mammalian cerebellar slices. *J Physiol* **305**, 171–195.

Llinas R & Yarom Y (1981*a*). Electrophysiology of mammalian inferior olivary neurones *in vitro*. Different types of voltage-dependent ionic conductances. *J Physiol* **315**, 549–567.

Llinas R & Yarom Y (1981*b*). Properties and distribution of ionic conductances generating electroresponsiveness of mammalian inferior olivary neurones *in vitro*. *J Physiol* **315**, 569–584.

Massaux A & Edeline JM (2003). Bursts in the medial geniculate body: a comparison between anesthetized and unanesthetized states in guinea pig. *Exp Brain Res* **153**, 573–578.

McCormick DA (1992). Neurotransmitter actions in the thalamus and cerebral cortex and their role in neuromodulation of thalamocortical activity. *Prog Neurobiol* **39**, 337–388.

Nowycky MC, Fox AP & Tsien RW (1985). Three types of neuronal calcium channel with different calcium agonist sensitivity. *Nature* **316**, 440–443.

Perez-Reyes E (2003). Molecular physiology of low-voltage-activated T-type calcium channels. *Physiol Rev* **83**, 117–161.

Ramcharan EJ, Gnadt JW & Sherman SM (2000). Burst and tonic firing in thalamic cells of unanesthetized, behaving monkeys. *Vis Neurosci* **17**, 55–62.

Sanchez-Vives MV & McCormick DA (2000). Cellular and network mechanisms of rhythmic recurrent activity in neocortex. *Nat Neurosci* **3**, 1027–1034.

Shah MJ, Meis S, Munsch T & Pape HC (2001). Modulation by extracellular pH of low- and high-voltage-activated calcium currents of rat thalamic relay neurons. *J Neurophysiol* **85**, 1051–1058.

Sharp AA, O'Neil MB, Abbott LF & Marder E (1993). The dynamic clamp: artificial conductances in biological neurons. *Trends Neurosci* **16**, 389–394.

Sherman SM (2001). Tonic and burst firing: dual modes of thalamocortical relay. *Trends Neurosci* **24**, 122–126.

Steriade M, Contreras D, Curro Dossi R & Nunez A (1993*a*). The slow (< 1 Hz) oscillation in reticular thalamic and thalamocortical neurons: scenario of sleep rhythm generation in interacting thalamic and neocortical networks. *J Neurosci* **13**, 3284–3299.

Steriade M, McCormick DA & Sejnowski TJ (1993*b*). Thalamocortical oscillations in the sleeping and aroused brain. *Science* **262**, 679–685.

Steriade M, Nunez A & Amzica F (1993*c*). Intracellular analysis of relations between the slow (< 1 Hz) neocortical oscillation and other sleep rhythms of the electroencephalogram. *J Neurosci* **13**, 3266–3283.

Steriade M, Nunez A & Amzica F (1993*d*). A novel slow (< 1 Hz) oscillation of neocortical neurons *in vivo*: depolarizing and hyperpolarizing components. *J Neurosci* **13**, 3252–3265.

Su H, Sochivko D, Becker A, Chen J, Jiang Y, Yaari Y *et al*. (2002). Upregulation of a T-type $Ca^{2+}$ channel causes a long-lasting modification of neuronal firing mode after status epilepticus. *J Neurosci* **22**, 3645–3655.

Swadlow HA & Gusev AG (2001). The impact of 'bursting' thalamic impulses at a neocortical synapse. *Nat Neurosci* **4**, 402–408.

Talley EM, Cribbs LL, Lee JH, Daud A, Perez-Reyes E & Bayliss DA (1999). Differential distribution of three members of a gene family encoding low voltage-activated (T-type) calcium channels. *J Neurosci* **19**, 1895–1911.

Timofeev I & Steriade M (1996). Low-frequency rhythms in the thalamus of intact-cortex and decorticated cats. *J Neurophysiol* **76**, 4152–4168.

Toth TI, Hughes SW & Crunelli V (1998). Analysis and biophysical interpretation of bistable behaviour in thalamocortical neurons. *Neuroscience* **87**, 519–523.

Tsakiridou E, Bertollini L, de Curtis M, Avanzini G & Pape HC (1995). Selective increase in T-type calcium conductance of reticular thalamic neurons in a rat model of absence epilepsy. *J Neurosci* **15**, 3110–3117.

Williams SR, Toth TI, Turner JP, Hughes SW & Crunelli V (1997). The 'window' component of the low threshold $Ca^{2+}$ current produces input signal amplification and bistability in cat and rat thalamocortical neurones. *J Physiol* **505**, 689–705.

Zhang Y, Mori M, Burgess DL & Noebels JL (2002). Mutations in high-voltage-activated calcium channel genes stimulate low-voltage-activated currents in mouse thalamic relay neurons. *J Neurosci* **22**, 6362–6371.

## Acknowledgements

Work supported by the Wellcome Trust.